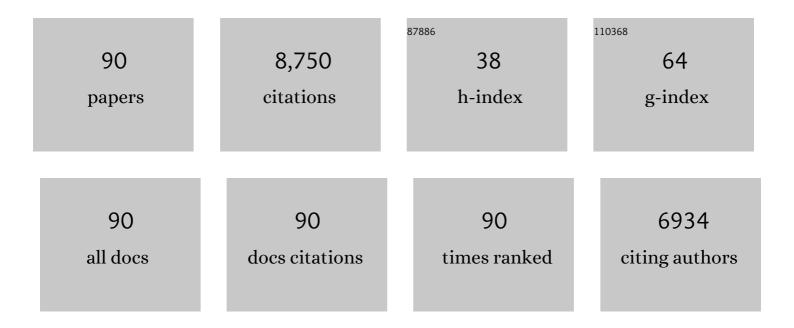
## **George Stoica**

List of Publications by Year in descending order

Source: https://exaly.com/author-pdf/1471617/publications.pdf Version: 2024-02-01



#	Article	IF	CITATIONS
1	New Zealand White Rabbits Effectively Clear Borrelia burgdorferi B31 despite the Bacterium's Functional <i>vlsE</i> Antigenic Variation System. Infection and Immunity, 2019, 87, .	2.2	6
2	Pleiotropic neuropathological and biochemical alterations associated with Myo5a mutation in a rat Model. Brain Research, 2018, 1679, 155-170.	2.2	14
3	Triplications of human chromosome 21 orthologous regions in mice result in expansion of megakaryocyte-erythroid progenitors and reduction of granulocyte-macrophage progenitors. Oncotarget, 2018, 9, 4773-4786.	1.8	4
4	Spontaneous multicentric soft tissue sarcoma in a captive African pygmy hedgehog ( <i>Atelerix) Tj ETQq0 0 889-895.</i>	0 rgBT /O 0.9	verlock 10 T 15
5	The pathogenesis of bornaviral diseases in mammals. Animal Health Research Reviews, 2016, 17, 92-109.	3.1	44
6	Cancer stem cells: Current status and future directions. Veterinary Journal, 2015, 205, 124-125.	1.7	1
7	Role of MMP2 in Brain Metastasis. Tumors of the Central Nervous System, 2014, , 195-205.	0.1	1
8	Metabolic Analysis of Striatal Tissues from Parkinson's Disease-like Rats by Electrospray Ionization Ion Mobility Mass Spectrometry. Analytical Chemistry, 2014, 86, 3075-3083.	6.5	20
9	MicroRNA profiling and the role of microRNA-132 in neurodegeneration using a rat model. Neuroscience Letters, 2013, 553, 153-158.	2.1	56
10	Potential role of αâ€synuclein in neurodegeneration: studies in a rat animal model. Journal of Neurochemistry, 2012, 122, 812-822.	3.9	29
11	Activation of AMP-activated protein kinase in cerebella of Atmâ^'/â^' mice is attributable to accumulation of reactive oxygen species. Biochemical and Biophysical Research Communications, 2012, 418, 267-272.	2.1	20
12	Curcumin induces apoptosis in a murine mammary gland adenocarcinoma cell line through the mitochondrial pathway. European Journal of Pharmacology, 2011, 668, 127-132.	3.5	24
13	Canine Astrocytic Tumors. Veterinary Pathology, 2011, 48, 266-275.	1.7	46
14	A mouse model of Down syndrome trisomic for all human chromosome 21 syntenic regions. Human Molecular Genetics, 2010, 19, 2780-2791.	2.9	197
15	Neuroprotective effects of the drug GVT (monosodium luminol) are mediated by the stabilization of Nrf2 in astrocytes. Neurochemistry International, 2010, 56, 780-788.	3.8	18
16	Effect of curcumin and Meriva on the lung metastasis of murine mammary gland adenocarcinoma. In Vivo, 2010, 24, 401-8.	1.3	17
17	Identification of Cancer Stem Cells in Dog Glioblastoma. Veterinary Pathology, 2009, 46, 391-406.	1.7	78
18	In-vivo photoacoustic microscopy of nanoshell extravasation from solid tumor vasculature. Journal of Biomedical Optics, 2009, 14, 010507.	2.6	110

#	Article	IF	CITATIONS
19	Attenuation of oxidative stress, inflammation and apoptosis by minocycline prevents retrovirus-induced neurodegeneration in mice. Brain Research, 2009, 1286, 174-184.	2.2	38
20	PRELIMINARY STUDY ON SKIN CANCER DETECTION IN SENCAR MICE USING MUELLER OPTICAL COHERENCE TOMOGRAPHY. Journal of Innovative Optical Health Sciences, 2009, 02, 289-294.	1.0	2
21	FGFâ€1â€induced matrix metalloproteinaseâ€9 expression in breast cancer cells is mediated by increased activities of NFâ€Î®B and activating proteinâ€1. Molecular Carcinogenesis, 2008, 47, 424-435.	2.7	48
22	Down-regulation of Jab1, HIF-1α, and VEGF by Moloney murine leukemia virus-ts1infection: A possible cause of neurodegeneration. Journal of NeuroVirology, 2008, 14, 239-251.	2.1	11
23	Simultaneous Molecular and Hypoxia Imaging of Brain Tumors <i>In Vivo</i> Using Spectroscopic Photoacoustic Tomography. Proceedings of the IEEE, 2008, 96, 481-489.	21.3	286
24	Up-regulation of pro-nerve growth factor, neurotrophin receptor p75, and sortilin is associated with retrovirus-induced spongiform encephalomyelopathy. Brain Research, 2008, 1208, 204-216.	2.2	18
25	In vivo burn imaging using Mueller optical coherence tomography. Optics Express, 2008, 16, 10279.	3.4	25
26	Limitations of quantitative photoacoustic measurements of blood oxygenation in small vessels. Physics in Medicine and Biology, 2007, 52, 1349-1361.	3.0	100
27	Photoacoustic imaging of lacZ gene expression in vivo. Journal of Biomedical Optics, 2007, 12, 020504.	2.6	161
28	Photoacoustic imaging of the microvasculature with a high-frequency ultrasound array transducer. Journal of Biomedical Optics, 2007, 12, 010501.	2.6	96
29	In vivo imaging and characterization of hypoxia-induced neovascularization and tumor invasion. International Journal of Oncology, 2007, 30, 45.	3.3	29
30	In-vivo imaging of nanoshell extravasation from solid tumor vasculature by photoacoustic microscopy. , 2007, , .		8
31	High-resolution burn imaging in pig skin by photoacoustic microscopy. , 2007, , .		3
32	Inherited tertiary hypothyroidism in Sprague–Dawley rats. Brain Research, 2007, 1148, 205-216.	2.2	13
33	MMP2 role in breast cancer brain metastasis development and its regulation by TIMP2 and ERK1/2. Clinical and Experimental Metastasis, 2007, 24, 341-351.	3.3	126
34	Three-dimensional imaging of skin melanoma in vivo by dual-wavelength photoacoustic microscopy. Journal of Biomedical Optics, 2006, 11, 034032.	2.6	242
35	Vascular Endothelial Growth Factor Stimulates Rat Cholangiocyte Proliferation Via an Autocrine Mechanism. Gastroenterology, 2006, 130, 1270-1282.	1.3	188
36	Improved in vivo photoacoustic microscopy based on a virtual-detector concept. Optics Letters, 2006, 31, 474.	3.3	167

#	Article	IF	CITATIONS
37	In vivo three-dimensional photoacoustic tomography of a whole mouse head. Optics Letters, 2006, 31, 2453.	3.3	43
38	In vivo volumetric imaging of subcutaneous microvasculature by photoacoustic microscopy. Optics Express, 2006, 14, 9317.	3.4	121
39	Imaging of gene expression in vivo with photoacoustic tomography. , 2006, , .		7
40	Photoacoustic molecular imaging of small animals in vivo. , 2006, , .		7
41	Burn depth determination using high-speed polarization-sensitive Mueller optical coherence tomography with continuous polarization modulation. , 2006, 6079, 421.		Ο
42	Three-dimensional photoacoustic imaging of subcutaneous microvasculature in vivo. , 2006, 6086, 365.		1
43	Functional photoacoustic microscopy in vivo. , 2006, 6086, 377.		1
44	Three-dimensional in vivo near-infrared photoacoustic tomography of whole small animal head. , 2006, 6086, 208.		0
45	In vivo functional photoacoustic tomography of traumatic brain injury in rats. , 2006, 6086, 201.		Ο
46	In vivo functional photoacoustic imaging of brain tumor vasculature. , 2006, 6086, 91.		1
47	Virtual-detector synthetic aperture focusing technique with application in in vivo photoacoustic microscopy. , 2006, 6086, 369.		1
48	Functional photoacoustic microscopy for high-resolution and noninvasive in vivo imaging. Nature Biotechnology, 2006, 24, 848-851.	17.5	1,690
49	Technical considerations in quantitative blood oxygenation measurement using photoacoustic microscopy in vivo. , 2006, 6086, 215.		14
50	Imaging acute thermal burns by photoacoustic microscopy. Journal of Biomedical Optics, 2006, 11, 054033.	2.6	83
51	Noninvasive imaging of hemoglobin concentration and oxygenation in the rat brain using high-resolution photoacoustic tomography. Journal of Biomedical Optics, 2006, 11, 024015.	2.6	400
52	Functional photoacoustic tomography for non-invasive imaging of cerebral blood oxygenation and blood volume in rat brain in vivo. , 2005, , .		1
53	Up-regulation of astrocyte cyclooxygenase-2, CCAAT/enhancer-binding protein, glucose-related protein 78, eukaryotic initiation factor 21±, and c-Jun N-terminal kinase by a neurovirulent murine retrovirus. Journal of NeuroVirology, 2005, 11, 166-179.	2.1	20
54	ATM deficiency induces oxidative stress and endoplasmic reticulum stress in astrocytes. Laboratory Investigation, 2005, 85, 1471-1480.	3.7	77

#	Article	IF	CITATIONS
55	Expression of MMP2, MMP9 and MMP3 in Breast Cancer Brain Metastasis in a Rat Model. Clinical and Experimental Metastasis, 2005, 22, 237-246.	3.3	182
56	Deep penetrating photoacoustic tomography in biological tissues. , 2005, , .		5
57	Photoacoustic tomography and molecular fluorescence imaging: dual modality imaging of small animal brains in vivo. , 2005, , .		6
58	Combined Photoacoustic and Molecular Fluorescence Imaging In Vivo. , 2005, 2006, 190-2.		10
59	Imaging of tumor angiogenesis in rat brains in vivo by photoacoustic tomography. Applied Optics, 2005, 44, 770.	2.1	189
60	Fiber-based polarization-sensitive Mueller matrix optical coherence tomography with continuous source polarization modulation. Applied Optics, 2005, 44, 5463.	2.1	43
61	Noninvasive functional photoacoustic tomography of blood-oxygen saturation in the brain. , 2004, 5320, 69.		13
62	High-resolution ultrasound-aided biophotonic imaging. , 2004, 2004, 5307-10.		1
63	Morphology, Immunohistochemistry, and Genetic Alterations in Dog Astrocytomas. Veterinary Pathology, 2004, 41, 10-19.	1.7	101
64	Possible involvement of both endoplasmic reticulum– and mitochondria-dependent pathways in MoMuLV-ts1–induced apoptosis in astrocytes. Journal of NeuroVirology, 2004, 10, 189-198.	2.1	48
65	Multiple-bandwidth photoacoustic tomography. Physics in Medicine and Biology, 2004, 49, 1329-1338.	3.0	200
66	Photoacoustic Tomography of a Nanoshell Contrast Agent in the in Vivo Rat Brain. Nano Letters, 2004, 4, 1689-1692.	9.1	447
67	Noninvasive photoacoustic angiography of animal brains in vivo with near-infrared light and an optical contrast agent. Optics Letters, 2004, 29, 730.	3.3	241
68	Determination of local polarization properties of biological samples in the presence of diattenuation by use of Mueller optical coherence tomography. Optics Letters, 2004, 29, 2402.	3.3	121
69	Activation of endoplasmic reticulum stress signaling pathway is associated with neuronal degeneration in MoMuLV-ts1-induced spongiform encephalomyelopathy. Laboratory Investigation, 2004, 84, 816-827.	3.7	40
70	Fiber-based polarization-sensitive Mueller-matrix optical coherence tomography with continuous source polarization modulation. , 2004, , .		1
71	Depth-wise differentiation of Jones matrices obtained from Mueller optical coherence tomography. , 2004, , .		0
72	Characterization of the polarization properties of biological tissues with fiber-based Mueller-matrix optical coherence tomography. , 2004, 5319, 130.		0

#	Article	IF	CITATIONS
73	Photoacoustic tomography of rat brain in vivo using multibandwidth ultrasonic detection. , 2004, , .		0
74	Laser-induced photoacoustic tomography enhanced with an optical contrast agent. , 2004, 5320, 77.		5
75	Noninvasive laser-induced photoacoustic tomography for structural and functional in vivo imaging of the brain. Nature Biotechnology, 2003, 21, 803-806.	17.5	1,597
76	Contrast mechanisms in polarization-sensitive Mueller-matrix optical coherence tomography and application in burn imaging. Applied Optics, 2003, 42, 5191.	2.1	75
77	Optical-fiber-based Mueller optical coherence tomography. Optics Letters, 2003, 28, 1206.	3.3	151
78	Three-dimensional laser-induced photoacoustic tomography of mouse brain with the skin and skull intact. Optics Letters, 2003, 28, 1739.	3.3	203
79	Laser-induced photoacoustic tomography for small animals. , 2003, 4960, 40.		4
80	Cancellation of the polarization distortions in fiber-based polarization-sensitive Mueller-matrix optical coherence tomography. , 2003, , .		0
81	Induction of p53 Accumulation by Moloney Murine Leukemia Virus-ts1 Infection in Astrocytes Via Activation of Extracellular Signal-Regulated Kinases 1/2. Laboratory Investigation, 2002, 82, 693-702.	3.7	24
82	Enhanced proteolysis of IκBα and IκBβ proteins in astrocytes by Moloney murine leukemia virus (MoMuLV)- ts 1 infection: A potential mechanism of NF-κB activation. Journal of NeuroVirology, 2001, 7, 466-475.	2.1	16
83	Clinical and pathologic aspects of spontaneous canine prostate carcinoma: A retrospective analysis of 76 cases. Prostate, 2000, 45, 173-183.	2.3	175
84	Effect of Intragastric Application ofN-Methylnitrosourea inp53 Knockout Mice. Molecular Carcinogenesis, 2000, 28, 97-101.	2.7	17
85	Interferon tau-induced hepatocyte apoptosis in sheep. Hepatology, 2000, 31, 1275-1284.	7.3	8
86	Neurodegeneration induced by MoMuLV-ts1 and increased expression of Fas and TNF-α in the central nervous system. Brain Research, 1998, 779, 1-8.	2.2	55
87	Mixed effects of 2,6-dithiopurine against cyclophosphamide mediated bladder and lung toxicity in mice. Toxicology, 1998, 125, 1-11.	4.2	13
88	Detection of Moloney murine sarcoma virus in tissues and cultured cells by the polymerase chain reaction. Journal of Virological Methods, 1993, 41, 255-263.	2.1	0
89	The role of the thymus in the pathogenesis of hind-limb paralysis induced by ts1, a mutant of moloney murine leukemia virus-TB. Virology, 1989, 169, 332-340.	2.4	27
90	In vitro malignant transformation of in vivo ENU-induced rat ovarian Sertoli cell tumor (adenoma). Journal of Cancer Research and Clinical Oncology, 1988, 114, 142-148.	2.5	4